Experimental study on the energy dissipation of foam concrete plate fragmentation under explosion loading

Wei Shang[a] , Xudong Zu[a]* , Zhengxiang Huang[a]* , Xin Jia[a] , Qiangqiang Xiao[a]

[a]School of Mechanical Engineering, Nanjing University of Science and Technology, Nanjing 210094, China. Email: ammosw0257@njust.edu.cn, zuxudong9902@njust.edu.cn, huangyu@mail.njust.edu.cn, jiaxinnjust@hotmail.com, xiaowawj@njust.edu.cn.

*Corresponding author

https://doi.org/10.1590/1679-78257141

Abstract

Fragmentation is the main energy dissipation form of foam concrete under explosion loading. To characterize the energy dissipation of foam concrete fragmentation quantitatively, explosion loading experiments of foam concrete plates under different stand-offs and plate thicknesses were carried out. The statistical characteristics of fragments and the energy dissipation law of foam concrete plate fragmentation were studied using image processing, fracture mechanics theory and fractal theory. An engineering calculation model of fragmentation fractal dimension and energy dissipation density of foam concrete plates were established. Results show that: the fragmentation of foam concrete plates under different explosion conditions is a fractal in the statistical sense. With the increase in stand-off and plate thickness, the fragment size of foam concrete plates increases, and the fragmentation fractal dimension decreases linearly. The linear relationship between the energy dissipation density and the fragmentation fractal dimension of foam concrete are expressed as $D_f = 0.0165\omega + 1.053$.

Keywords

Explosion loading; Foam concrete plate; Energy dissipation; Fragmentation fractal dimension.

Graphical Abstract
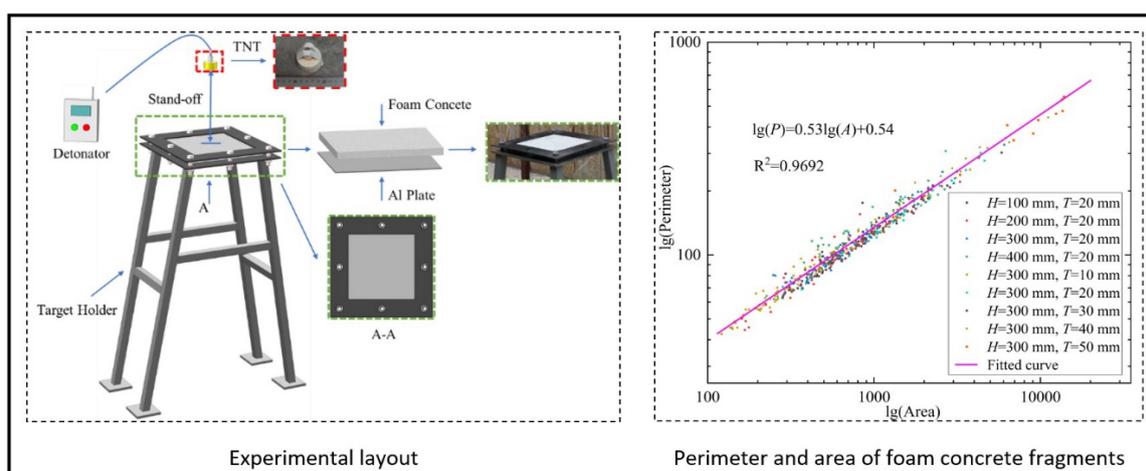
Experimental layout

Perimeter and area of foam concrete fragments

1 INTRODUCTION

Foam concrete is a lightweight porous concrete with a closed cell structure. This type of concrete has cement as its main gel material and introduces bubbles into the slurry made of aggregate, admixture, and water (Ramamurthy et al., 2009). Owing to the porous and fragile characteristics, foam concrete has been widely used as the energy dissipation layer of building wallboards, airport runways, underground tunnels and other engineering facilities to reduce the damage effect of external loads on the primary structure (Shen et al., 2014; Zhang and Yang, 2015; Zhao et al., 2013). In the above engineering applications, how to characterize the energy dissipation of foam concrete is an important topic of structural safety design.

The energy dissipation mechanism of foam concrete is the foundation of its engineering application, and related researches have been widely concerned by scholars. Through shock tube experiments, Kolluru (2013), Nian et al. (2016) et al. found that when foam concrete specimens were placed in the loading path of explosion wave, the specimens would be crushed, and stress would be transferred to subsequent structures. The amplitude of transferred stress was related to the specimen length. Alhadid et al. (2014), Edward et al. (2012). Analyzed the microstructural characteristics of foam concrete and concluded that the existence of pores makes foam concrete fragile. When explosion loaded, the fragmentation of foam concrete would dissipate substantial energy, and the mass and velocity of spalling fragments were significantly lower than those of traditional concrete, thus reducing the secondary damage to personnel and equipment caused by fragments. Wang et al. (2021), Tian et al. (2016). Studied the dynamic response of foam concrete plates with different structural parameters under explosion loading, and concluded that load strength, the thickness, density, and compressive strength of foam concrete are the main factors affecting its cushioning effect. The above researches show that fragmentation is the main energy dissipation form of foam concrete structures under explosion loading, and the fragmentation of foam concrete is related to load strength and structural parameters. However, the characterization of energy dissipation in fragmentation is mostly reflected by indirect parameters such as the attenuation of stress wave amplitude and the damage of protected structure. A unified evaluation standard for guiding structural explosion-proof design has not been formed. Therefore, the energy dissipation of foam concrete fragmentation must be quantified directly.

The relationships between fragment number, fragment size, and energy dissipation are the basic problem in fragmentation. To characterize the energy dissipation in fragmentation quantitatively, the fragment size distribution law must be first obtained (Hu and Wittmann, 1992; Grady, 1990). Carpinteri et al. (2004) analyzed numerous of concrete fragmentation experiments to evaluate the influence of fragment size on energy dissipation density. Results indicated that the size distribution of fragments conformed to the fractal law. The fractal concept allowed to quantify the correlation between fragment size distribution and energy dissipation density. Ji J. et al. (2020) obtained the size distribution curve of rock fragments under different strain rates through split Hopkinson pressure bar (SHPB) experiments, calculated the rock fragmentation energy on the basis of energy transfer relationship in the SHPB experiments, and established the quantitative relationship between rock fragmentation fractal dimension, loading parameters, and energy dissipation. Results showed that the fractal dimension of rock fragmentation and the energy dissipation density increase with the increase in strain rate, and the relationship between them satisfies the power function. Li et al. (2021) studied the effects of loading rate and aggregate volume fraction on the fractal fracture characteristics of concrete through SHPB experiments and established the analytical expressions of fragmentation fractal dimension and crack surface energy on the basis of fracture theory. Results indicated that the fractal dimension, energy dissipation in fragmentation and crack surface energy increase with the increase in impact velocity and decrease with the increase in aggregate volume ratio. Lei et al. (2021) established an energy dissipation calculation model of rock fragmentation based on the fragment size distribution law after explosion and studied the influence of minimum resistance line on rock energy dissipation. Results showed that the fragmentation fractal dimension and energy dissipation density of rock decrease linearly with the increase in resistance line. Xu et al. (2019) calculated the fragment size of the rock near the explosion zone on the basis of rock fracture theory and established the corresponding relationship between the fractal dimension and the blasting damage. Results provided the possibility for the prediction of the blasting damage. The above research shows that the fractal dimension of fragmentation has correlations with the fragmentation degree and energy dissipation. The larger the fractal dimension is, the smaller the average size of fragments is. Fractal requires the objects to be studied to have self-similarity (Turcotte,1986). Kim et al. (2020) observed the microstructural characteristics of foam concrete through micro-CT and proved the correlation between its mechanical behavior and microstructure in accordance with the numerical simulation results. Chao et al. (2021) proved the self-similarity of the mechanical properties of random porous materials on the basis of fractal theory. Feng et al. (2020) studied the damage characteristics of foam concrete under impact loading through SPHB experiments. Results showed that the damage mode of foam concrete under different strains conformed to fractal characteristics. The above

research only proves the self-similarity of foam concrete in microstructure, mechanical properties and damage mode. The fragmentation of foam concrete structure under explosion loading is the result of crack formation and propagation. Whether the energy dissipation can be quantitatively characterized using fractal methods remains to be studied.

Aiming at the quantitative characterization of energy dissipation in foam concrete fragmentation under explosion loading, this study carried out explosion loading experiments of foam concrete plates under different stand-offs and plate thicknesses. The dynamic fragmentation process, statistical size characteristics of fragments and energy dissipation law of foam concrete plates fragmentation under explosion loading were systematically studied using fracture mechanics, image processing and fractal theory. Furthermore, an engineering calculation model of foam concrete fragmentation fractal dimension and energy dissipation was established.

2 EXPERIMENTAL MATERIALS AND SCHEME

2.1 Foam concrete

The ratio of cement, water and foaming agent in foam concrete was 20:8:1 in this study. As shown in Figure 1, foam concrete specimens were prepared in accordance with the pouring process and curing conditions specified in the experimental standards to test the basic mechanical properties of the material (GB/T 50081, 2019; ASTM. E756-05, 2017; ASTM. E1820-11, 2012). The test results of the main physical and mechanical parameters of foam concrete are shown in Table 1.
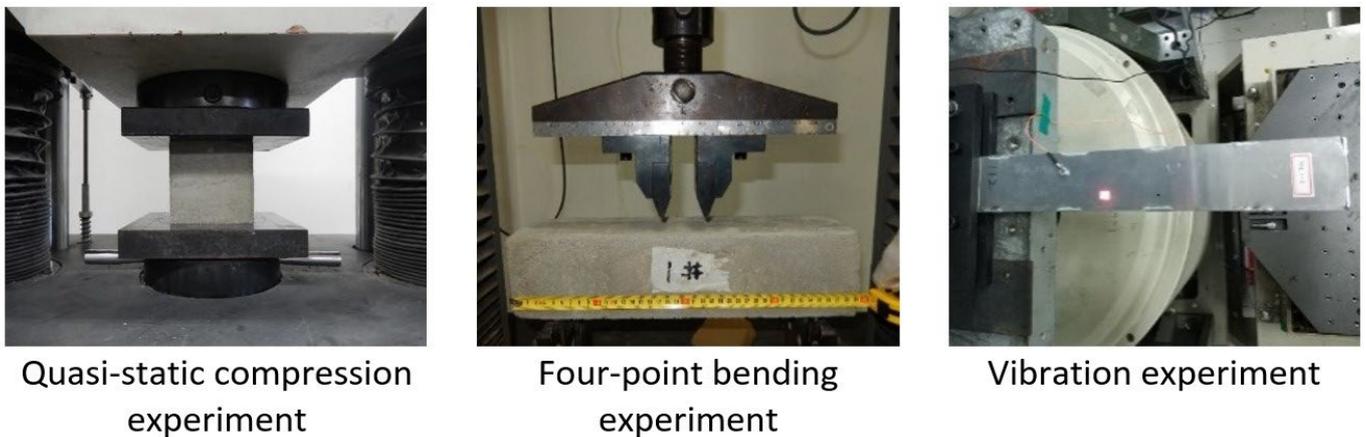

Quasi-static compression experiment

Four-point bending experiment

Vibration experiment

Figure 1 Mechanical properties test of foam concrete

Table 1 Main physical and mechanical parameters of foam concrete

Density ($\mathrm{g/cm^3}$)	Elastic modulus (MPa)	Poisson's ratio	Compressive strength (MPa)	Fracture toughness ($\mathrm{MPa \cdot m^{0.5}}$)	Damping ratio
0.82	880	0.2	4.4	0.35	0.1

2.2 Explosion experimental scheme

Cylindrical TNT charge was used in the explosion experiment, the charge mass was 50 g, and the basic size of the charge was Ф 40 mm × 26 mm. During the experiment, the explosive was detonated using 8# fire detonator and 2.5 g of passivated RDX. The foam concrete plates were square with a side length of 300 mm. Given that the foam concrete plates in building structures are fragmented under the constraint of bottom, to simulate the actual fragmentation process of foam concrete, 2A12 aluminum alloy with the closest wave impedance to the concrete was selected as the constraint material. The thickness of the aluminum alloy plate was 3 mm. The foam concrete and the aluminum alloy plate were bonded using a thin layer of epoxy resin adhesive. During the experiments, the target plate was clamped between two hollow steel plates, and the effective contact area between the foam concrete plate and the explosion wave was 260 mm × 260 mm. The upper and lower steel plates were connected by bolts to realize four-edge clamping of the target plate. The experimental layout of the test is shown in Figure 2. Table 2 presents the explosion experimental condition design. A total of nine explosion experiments were carried out by changing the stand-off and plate thickness. Experimental conditions 3 and 6 were repeated experiments.
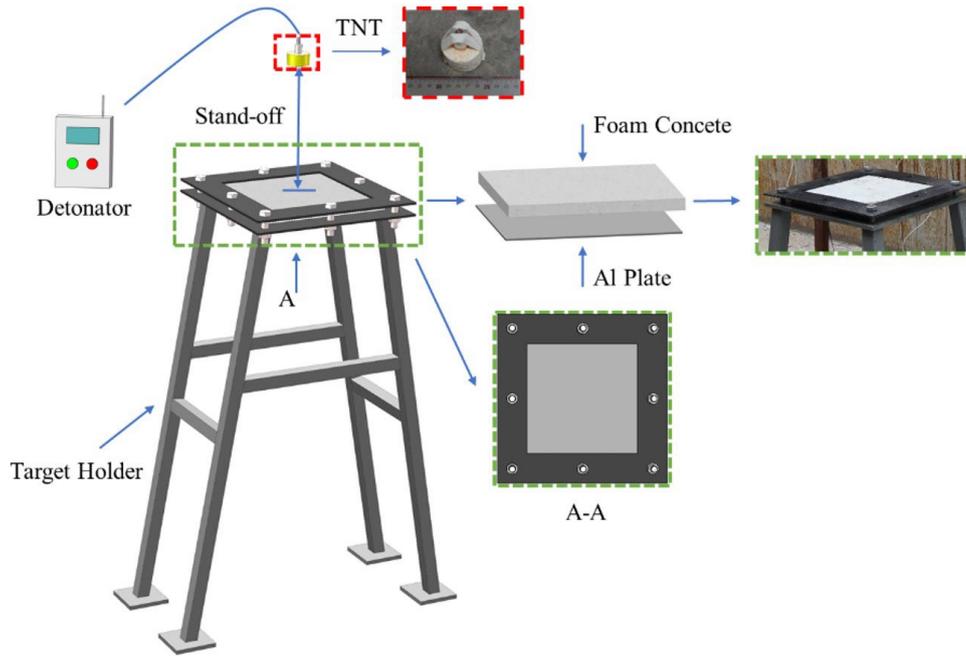
Figure 2 Experimental layout

Table 2 Explosion experimental conditions

Experimental number	Explosive parameters	Stand-off (mm)	Foam concrete plate	
			Basic dimensions (mm)	Mass (g)
1		100		
2		200		
3		300	300×300×20	1440
4	Type: TNT	400		
5	Dimensions: Φ40 mm×26 mm		300×300×10	720
6	Mass: 50 g		300×300×20	1440
7		300	300×300×30	2160
8			300×300×40	2880
9			300×300×50	3600

2.3 Experimental condition analysis

When the bottom surface is constrained by an aluminum plate, the motion of the foam concrete plate can be described by the Winkler elastic foundation plate motion equation (Wang et al., 2005):

$$D\nabla^4 w(x,y,t) + \rho T \frac{\partial^2 w(x,y,t)}{\partial t^2} = p(x,y,t) - kw(x,y,t),$$ (1)

Where ρ is the density of foam concrete, T is the plate thickness, $D = \frac{ET^3}{12(1-v^2)}$ is the bending stiffness of the foam

concrete plate, $p(x,y,t)$ is the load distribution on the blasting face of the foam concrete plate, w is the deformation deflection of the foam concrete plate, and k is the elastic coefficient of the aluminum plate.

In accordance with the modified Friedlander formula, the explosion loading on any point of the plate surface can be expressed as (Fu and Zhang, 2007):

$$p(x,y,t) = \frac{3\gamma-1}{\gamma-1} p_{pos} \frac{H}{R}\left(1 - \frac{t}{t_{pos}}\right) e^{-\beta\frac{t}{t_{pos}}},$$ (2)

where γ is the adiabatic index of air; $\gamma = 1.4$. $R(x,y) = \sqrt{(x-x_0)^2 + (y-y_0)^2 + H^2}$, where (x_0, y_0) is the projection of explosion center on the blasting face of the foam concrete plate. H is the stand-off. p_{pos} , t_{pos} , and β are the overpressure, duration, and decay parameter of the explosion wave, which can be calculated using the Kinney - Graham formula (Kinney and Grahm, 1985).

The boundary condition of the foam concrete plate with four-edge clamping can be expressed as:

$$w(0,y,t) = w(a,y,t) = w(x,0,t) = w(x,a,t) = 0 \tag{3.1}$$

$$\frac{\partial w}{\partial x}(0,y,t) = \frac{\partial w}{\partial x}(a,y,t) = \frac{\partial w}{\partial y}(x,0,t) = \frac{\partial w}{\partial y}(x,a,t) = 0 \tag{3.2}$$

where a is the side length of the foam concrete plate.

From the analysis of the movement of foam concrete plates under experimental conditions, when the explosive equivalent, material and constraint conditions are determined, the deformation deflection of foam concrete plate is only related to the stand-off and plate thickness.

3 EXPERIMENTAL RESULTS AND ANALYSIS

3.1 Fragmentation process and phenomenon

The fragmentation of foam concrete plates under explosion loading is a complex dynamic process. In this process, the foam concrete plate is assumed to be always in a plane stress state. In accordance with the geometric equation, the nonzero strain component of each point in the plate can be expressed as (Rudolph, 2004):

$$\begin{cases} \varepsilon_x = \dfrac{\partial u}{\partial x} = -z\dfrac{\partial^2 w}{\partial x^2} \\[2mm] \varepsilon_y = \dfrac{\partial v}{\partial y} = -z\dfrac{\partial^2 w}{\partial y^2} \\[2mm] \gamma_{xy} = \dfrac{\partial u}{\partial y} + \dfrac{\partial v}{\partial x} = -2z\dfrac{\partial^2 w}{\partial x \partial y} \end{cases} \tag{4}$$

Through substituting Equation (4) into the physical equation of elasticity, the relationship between the main stress component and deflection in the plate can be derived as (Rudolph, 2004):

$$\begin{cases} \sigma_x = -\dfrac{Ez}{1-v^2}\left(\dfrac{\partial^2 w}{\partial x^2} + v\dfrac{\partial^2 w}{\partial y^2}\right) \\[3mm] \sigma_y = -\dfrac{Ez}{1-v^2}\left(\dfrac{\partial^2 w}{\partial y^2} + v\dfrac{\partial^2 w}{\partial x^2}\right) \\[3mm] \tau_{xy} = -\dfrac{Ez}{1+v}\dfrac{\partial^2 w}{\partial x \partial y} \end{cases} \tag{5}$$

The fracture of the foam concrete plate is assumed to obey the von Mises yield criterion, i.e:

$$(\sigma_x - \sigma_y)^2 + (\sigma_y - \sigma_z)^2 + (\sigma_z - \sigma_x)^2 = 2\sigma^2 \tag{6}$$

σ_d represents the dynamic strength of foam concrete. When $\sigma > \sigma_d$ is satisfied, the crack begins to propagate.

The directions of stress and crack growth on the foam concrete plate are related to the process of shock and stress wave propagation. First, the shock wave generated by explosion is loaded on the center of the foam concrete plate

instantaneously, exerting a strong compression effect on the plate. When the strength of the shock wave is greater than the compressive strength of foam concrete, the foam concrete is crushed. The crushing zone dissipates shock wave energy and attenuates the shock wave at the interface into a stress wave. The compression wave continues to propagate along the radial direction in the plate. After the stress wave, compressive stress is generated in the radial direction, while tensile stress is generated in the tangential direction. Given that the tensile strength of foam concrete is considerably less than the compressive strength, when the tangential tensile stress is greater than the tensile strength of foam concrete, the foam concrete will be pulled off, forming radial cracks connected to the crushing zone. Simultaneously, the foam concrete is strongly compressed and accumulates a large amount of elastic deformation energy under the shock and stress wave loading. With the cavity formation in the crushing zone and the radial crack propagation, when the pressure drops rapidly to a certain extent, the elastic deformation energy accumulated in the foam concrete near the plate center will be released and transformed into an unloading wave. This wave forms a centripetal tensile stress opposite to the compressive stress wave, and results in a reverse radial movement of the foam concrete fragments. When the centripetal tensile stress is greater than the tensile strength of foam concrete, the foam concrete is pulled to fracture and generates a circumferential crack. Shear cracks also generates as a result of the superposition of radial stress and tangential stress. The initial crack is generated under stress wave loading, and then the escape of detonation gas promotes the crack extension. The crack propagation stops only when the stress wave and detonation gas decay to a certain extent. As shown in Figure 3, the fragmented foam concrete plate is distributed with central crushing zone, radial crack and circumferential crack. Along the central crushing zone to the edge of the plate, there are three typical shapes of fragments, i.e, approximate right triangle, right trapezoid, and rectangle. The hypotenuses of the first two shapes of fragments are shear fractures close to 45 °, and each edge of the latter shape of fragments presents tensile fractures. The experimental results verify the analysis of the fragmentation process of foam concrete plates based on plate fracture theory.
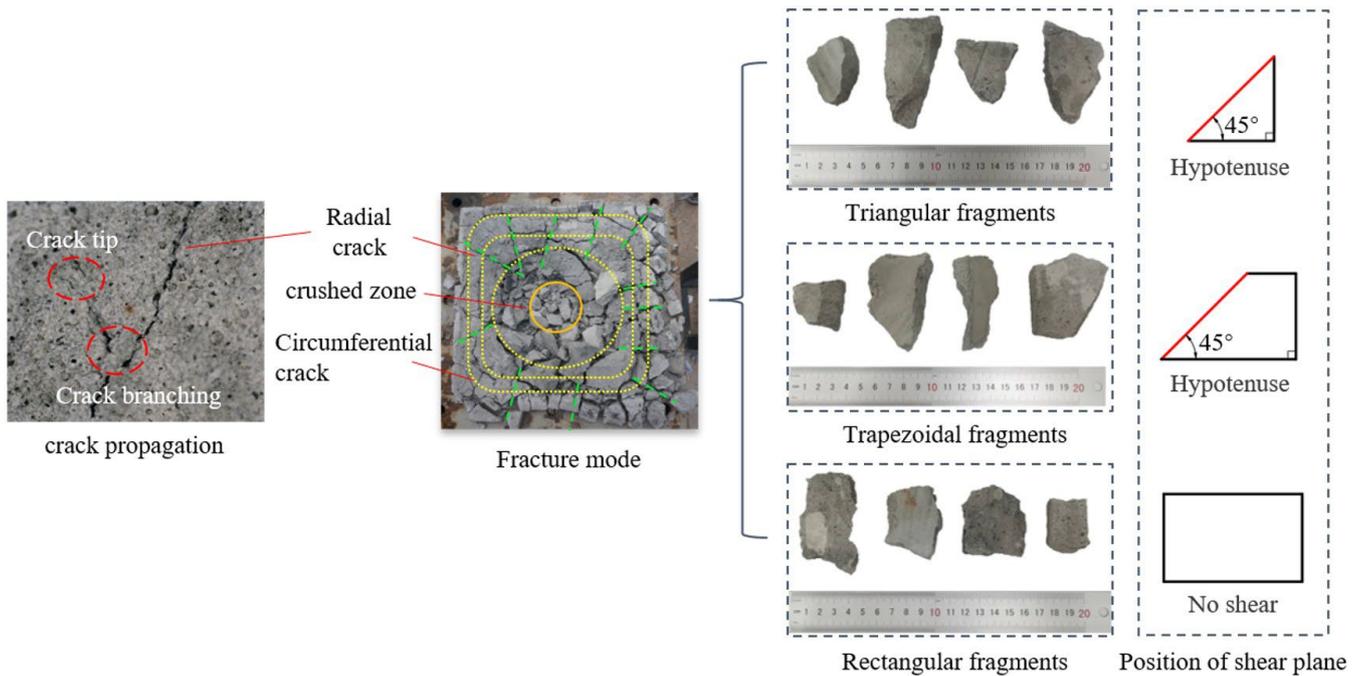

Figure 3 Analysis of fragmentation process and fracture morphology of foam concrete

Among the above cracks, the radial and circumferential cracks are type I cracks, and the stress at the attachment of the crack tip is (Alan, 2012):

$$\begin{Bmatrix} \sigma_x \\ \sigma_y \\ \tau \end{Bmatrix} = \frac{K_{IC}}{\sqrt{2\pi c}} \cos\frac{\theta}{2} \begin{Bmatrix} 1 - \sin\frac{\theta}{2}\sin\frac{3}{2}\theta \\ 1 + \sin\frac{\theta}{2}\sin\frac{3}{2}\theta \\ \sin\frac{\theta}{2}\cos\frac{3}{2}\theta \end{Bmatrix} \tag{7}$$

The shear cracks are type II cracks, and the stress near the crack tip is (Alan, 2012):

$$\begin{Bmatrix} \sigma_x \\ \sigma_y \\ \tau \end{Bmatrix} = \frac{K_{\mathrm{IC}}}{\sqrt{2\pi c}} \begin{Bmatrix} -\sin\dfrac{\theta}{2}\left(2+\cos\dfrac{\theta}{2}\cos\dfrac{3}{2}\theta\right) \\ \sin\dfrac{\theta}{2}\cos\dfrac{\theta}{2}\cos\dfrac{3}{2}\theta \\ \cos\dfrac{\theta}{2}\left(1-\sin\dfrac{\theta}{2}\sin\dfrac{3}{2}\theta\right) \end{Bmatrix} \tag{8}$$

where, K_{IC} is the fracture toughness of foam concrete. c is the distance from the crack tip to any point, and θ is the direction angle between c and the crack surface.

Figures 4 and 5 show the fracture and fragmentation of foam concrete plates under different stand-offs and thicknesses respectively. In terms of fracture morphology, when the stand-off or the plate thickness is small, the foam concrete plate is fragmented as a whole and flied out when the aluminum plate vibrates, so the crack propagation process cannot be observed. When the stand-off or plate thickness increases, a crushing zone exists at the center of the foam concrete plate, and the fragments tend to fly outward. Radial, circumferential and shear cracks are distributed outside the crushing zone. The staggered crack network divides the foam concrete plate into fragments of different sizes. As the plate thickness or stand-off further increases, the foam concrete plate becomes dominated by crack propagation, without an obvious crushing zone. When the plate thickness is 50 mm, only radial cracks appear on the plate plane. In terms of fragment size, it gradually increases with the increase in stand-off and thickness. On the same plate, the fragment size near the central area is small, and it gradually increases outward along the radial direction.
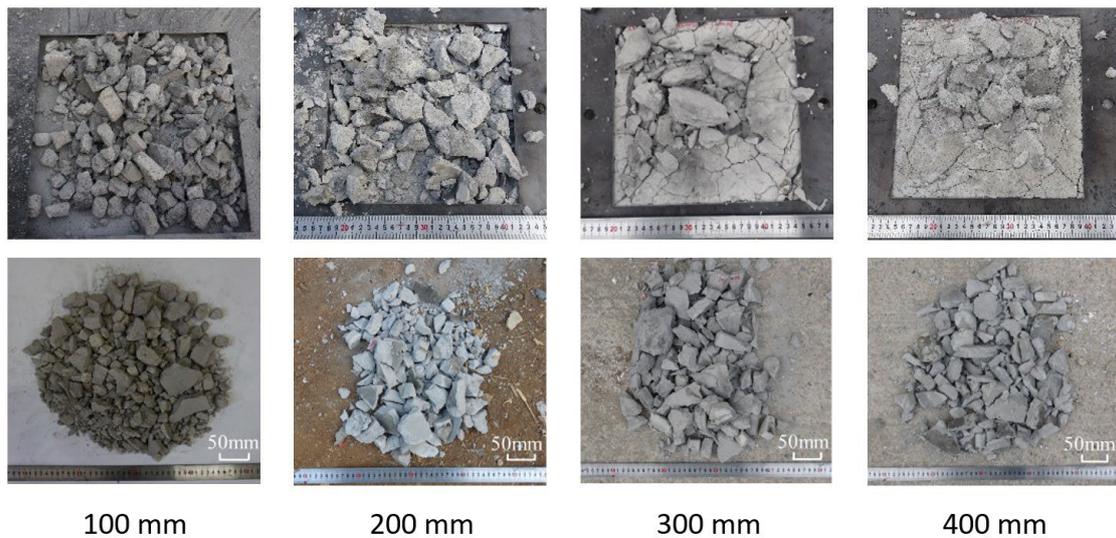

| 100 mm | 200 mm | 300 mm | 400 mm |

Figure 4 Fracture and fragmentation of foam concrete plates with different stand-offs (the plate thickness is 20mm)
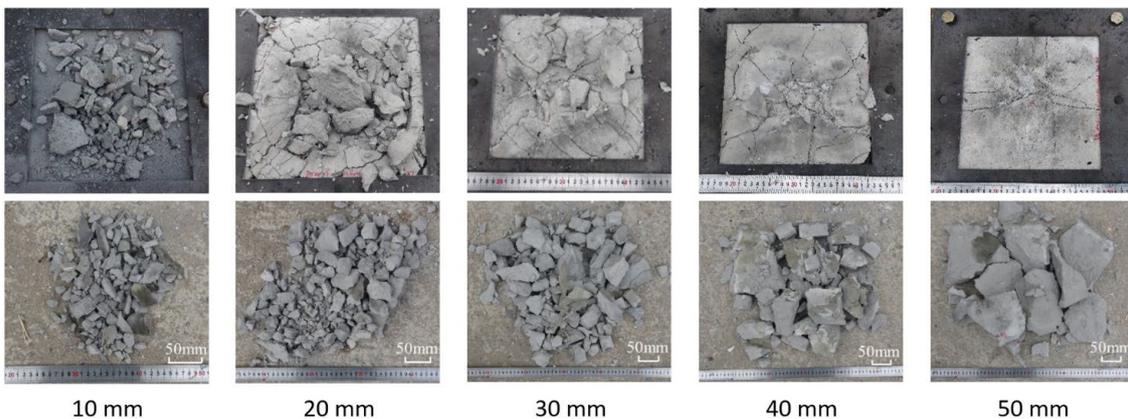

| 10 mm | 20 mm | 30 mm | 40 mm | 50 mm |

Figure 5 Fracture and fragmentation of foam concrete plates with different plate thicknesses (the stand-off is 300 mm)

3.2 Statistical analysis of fragmentation

The image processing method is used to analyze the foam concrete fragments generated in explosion statistically. The detailed steps are shown in Figure 6. First, the original images of fragment are preprocessed to simplify the image background. Then, the LabelMe software is used to label the preprocessed fragment images and make the image sample set. Next, the DeepLab V3 + network is used to learn the preprocessed and labeled images deeply, and each pixel of the preprocessed image is associated with the corresponding labeled image. The model file obtained through the above steps can realize rapid labeling of fragment images. After labeled images containing pixel information are obtained, the im2bw function in MATLAB is used to convert a labeled image into a binary image. Lastly, the regionprops function is used to return the number, pixel values of maximum/small diameter, perimeter, and area of foam concrete fragments in the binary image. In accordance with the proportional relationship between the pixel value and the real value, the real size of the fragments can be converted, as shown below:

$$\frac{f_t}{f_p} = \frac{f_{rt}}{f_{rp}} \tag{9}$$

where f_t and f_p respectively represent the real value and pixel value of the fragments, and f_{rt} and f_{rp} respectively represent the real value and pixel value of the reference object. The preprocessing of original images is the key step, which requires that the image background should not be too complex, and the shadow or overlap at the fragment boundary should be avoided as much as possible. Practice shows that the image processing method has a poor recognition effect on the fragments with sizes less than 20 mm because smaller foam concrete fragments have a large number and are densely distributed, and the fragment boundary is difficult to identify. In this study, only the foam concrete fragments with size greater than or equal to 20 mm are counted.
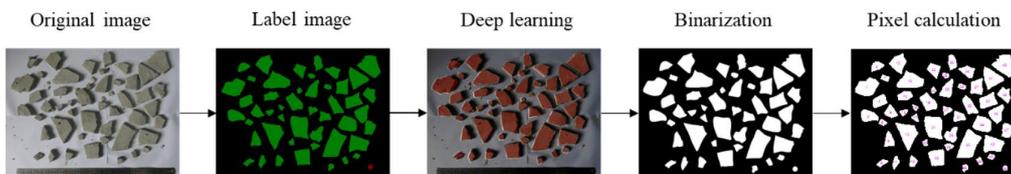

Figure 6 Image processing flow of experimental results

The average values of the maximum/minimum diameters of foam concrete fragments are calculated, and the results are shown in Figures 7 and 8. With the increase in stand-off and plate thickness, the size of foam concrete fragments after explosion tends to increase gradually. For every 100 mm increase in stand-off, the maximum average size of foam concrete fragments increases by about 11.2%. For every 10 mm increase in thickness, the maximum average size of foam concrete fragments within the thickness range of 10 - 40mm increases by about 25.7%. The size of foam concrete fragments increases significantly when the thickness is 50 mm, the change may be related to the conversion of fracture morphology. Under this experimental condition, no circumferential crack is generated on the surface of the foam concrete plate. Comparison of the average size of fragments under different experimental conditions shows the ratio of the maximum average size to the minimum average size of foam concrete fragments is 1.57 ± 0.12.
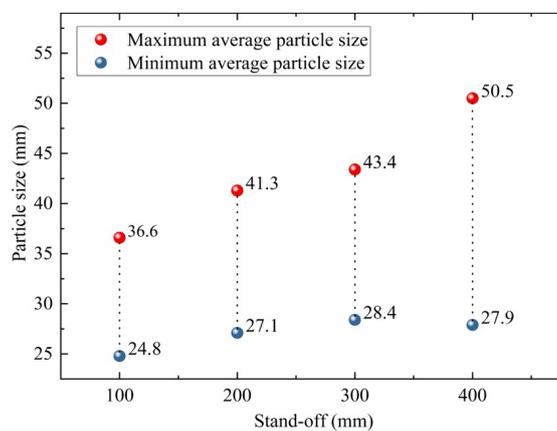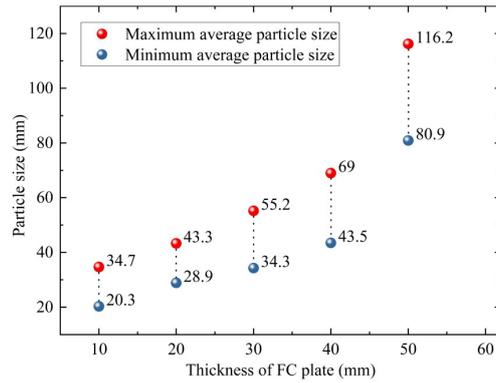

**Figure 7** Fragments size of foam concrete plates with different stand-offs

Figure 8 Fragments size of foam concrete plates with different thicknesses

When brittle materials are fragmented under explosion loading, the statistical characteristics of fragments are often described by the Weibull distribution of two parameters. The expression of Weibull distribution is (Shi et al., 2020):

$$f(r) = 1 - \exp\left[-\left(\frac{r}{r^*} \right)^N \right] \tag{10}$$

where, r represents the size of fragments, and $f(r)$ represents the proportion of the fragments feature quantity whose size is less than r in the corresponding overall feature quantity. r^* is the relative size of fragments and N is the shape parameter of the function, which can be fitted using the experimental data.

Equation (10) is used to fit the area distribution characteristics of the fragments on the plate plane after fragmentation. The total area of the fragments on the plate plane is 300 mm × 300 mm. As shown in Figures 9 and 10, the fitted results indicate that the Weibull distribution of two parameters can well describe the cumulative probability of the area of foam concrete fragments with the fragment size.
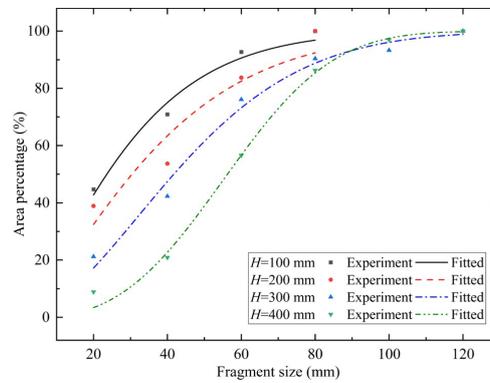
Figure 9 Cumulative probability of fragments area of foam concrete with different stand-offs
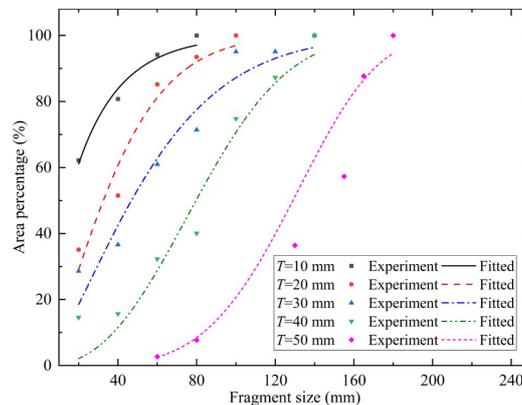
Figure 10 Cumulative probability of fragment area of foam concrete with different plate thicknesses

3.3 Calculation of energy dissipation

Rittinger's surface area theory states that the fragmentation process produces fragments of different sizes. Each fragmentation step increases the number of fragments, which also increases new fracture surface to dissipate more energy. The energy required for fragmentation is directly proportional to the new surface area in fragmentation. Therefore, the energy dissipated to generate new surfaces in the fragmentation of the foam concrete plate is (Xu et al., 2019):

$$E_v = 2K_{IC}^2 A_b / E \tag{11}$$

where E_v is the energy required to generate new surfaces, that is, the energy dissipated in fragmentation. A_b is the area of the newly added surface, and E is the elastic modulus of foam concrete.

Fragment size distribution is the macroembodiment of energy consumption in fragmentation. Different fragmentation has diverse sizes of new surface area. Given that the stress change along the thickness direction of the foam concrete plate is not considered, the new surface area of each irregularly shaped fragment is:

$$A_i = P_i \cdot T \tag{12}$$

where A_i and P_i represent the new surface area and the perimeter of fragments.

For the whole plate, the new surface area after fragmentation is:

$$A_b = \left(\sum A_i - 4a \cdot T \right) / 2 \tag{13}$$

When the size parameters of fragments are calculated, the perimeter of fragments with size greater than or equal to 20 mm and the proportion of fragments with size less than 20 mm have been obtained. Assuming that the maximum average size of fragments with size less than 20 mm is 10 mm, the ratio of the maximum average size to the minimum average size is set to 1.57 in accordance with the statistical results. Therefore, fragments with sizes less than 20 mm are equivalent to cuboids. The length and width of the cuboids are 10 mm × 6.4 mm and the height of the cuboids is equal to the thickness of the plate. The new surface area of the whole fragmented plate can be calculated using Equation (13), and the energy dissipation in fragmentation can be calculated by substituting the new surface area into Equation (11). Based on Rittinger's theory, this method quantifies the energy dissipation of foam concrete plates in fragmentation through the interrelations among fragment size distribution, new surface area and energy dissipation. The calculation results are shown in Table 3. The results indicate that the energy dissipation and the energy dissipation density of foam concrete in fragmentation decrease with the increase in stand-off. With the increase in plate thickness, the energy dissipation first increases and then decreases, and the energy dissipation density gradually decreases. At 300 mm stand-off, the plate thickness corresponding to the maximum energy dissipation is 30mm. Under this thickness, the energy dissipation efficiency of the foam concrete plate is the highest.

Table 3 Calculation results of energy dissipation in fragmentation

Experimental number	New area (cm²)	Dissipation energy (J)	Fragmentation volume (cm³)	Dissipation energy density ($\mathrm{KJ \cdot m^{-3}}$)
1	5563.3	154.9	1800	86
2	4923.9	137.1	1800	76.2
3	3710.7	118.1	1800	65.6
4	2981.1	84.5	1800	44.7
5	3352.7	93.3	900	103.7
6	4668.4	130	1800	72.2
7	5908.2	164.5	2700	60.9
8	5461.1	152	3600	42.2
9	2162.5	60.2	4500	13.4

4 FRACTAL FRAGMENTATION CHARCTERISTICS

4.1 Fractal of dynamic fragmentation process

The macrofragmentation of the foam concrete plate is the final result of the continuous development, propagation, aggregation and penetration of its internal micro cracks. The process from microdamage to macrofragmentation is an energy dissipation process. The internal mesocracks and pores have self-similarity at different scales, and the fragmentation process and fragment shape are the direct result of crack propagation. These self-similarity behaviors will inevitably lead to the self-similarities of fragment size and energy dissipation, which are a fractal in a statistical sense (Xie, 1996). The fractal characteristics of fragment size distribution are closely related to the mesostructure, loading mode, shape, and size of foam concrete members, which is a comprehensive reflection of these factors (Yang et al., 1999). Figure 11 shows a group of foam concrete fragments collected in the experiments. It can be found that fragments of different sizes on the same plate have self-similarity. The ratio of the maximum average size to the minimum average size of each group of fragments in Figures 7 and 8 is close to 1.57, which proves that the fragmentation of foam concrete plates under different explosion conditions has self-similarity.

Figure 11 Size distribution of foam concrete fragments(400 mm stand-off / 20 mm plate thickness)

According to the fractal fracture mechanics, the perimeter of the fracture surface generated on the foam concrete plate is infinite, but the area is limited. If the fragment size distribution meets the fractal characteristics, its perimeter and area shall meet the following relationship (Xie, 1996):

$$P^{1/B} \sim A^{1/2} \tag{14}$$

where P is the non-standard (fractal) perimeter, A is the area of standard plane (European style), and B is the self-similar parameter of different fault planes. B can be obtained from Equation (14) as

$$\log(P) = C + \frac{B}{2}\log(A) \tag{15}$$

That is, the double logarithmic line of fragment perimeter and area data is a straight line, and the slope of the straight line is $B/2$. C is a constant.

The perimeter and area data of foam concrete fragments measured under different experimental conditions are plotted in double logarithmic coordinates, and the results are shown in Figure 12. All the data points approximately fall on the same straight line, which proves that the fragments generated by explosion loading on the foam concrete plate have fractal characteristics.
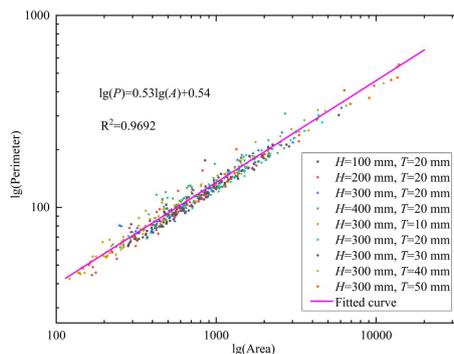
Figure 12 Perimeter and area distribution of foam concrete fragments

4.2 Calculation of fractal dimension of fragmentation

Fractal dimension is an appropriate measurement of the degree of fragmentation of the specimen. A specimen with a large fractal dimension has a high fragmentation degree, and the generated fragments have the characteristics of large quantity and small size. A specimen with a small fractal dimension has a low fragmentation degree, and the generated fragments have the characteristics of small quantity and large size (Xu and Fan, 2012). The fractal dimension can be obtained from the mass–frequency relationship of fragments. The fragment distribution equation of a foam concrete plate under explosion loading is (Turcotte, 1986):

$$\frac{M_{(r)}}{M} = \left(\frac{r}{r_m}\right)^{3-D_f} \tag{16}$$

where D_f is the fragmentation fractal dimension, and M and $M_{(r)}$ respectively represent the total mass of fragments and the cumulative mass of fragments with sizes smaller than r. r_m represents the maximum size of the fragments. $M_{(r)}$ can be calculated from the cumulative probability of fragment area with fragment size, i.e,

$$M_{(r)} = a^2 \cdot f(r) \cdot \rho \cdot T \tag{17}$$

Take logarithms on both sides of Equation (16) are considered to obtain

$$\lg(M_{(r)}/M) = (3 - D_f)\lg(r/r_m) \tag{18}$$

Equation (18) shows that the slope of the fitted line in the double logarithmic coordinate system $\lg(M_{(r)}/M)$ - $\lg(r)$ is $(3 - D_f)$. The experimental results under different conditions are plotted in the double logarithmic coordinate system and fitted linearly. The fitted results are shown in Figures 13 and 14. Table 4 presents the calculation results of fractal dimension. When the stand-off is in the range of 100–400 mm, the value of fractal dimension is reduced from 2.40 to 1.53. When the thickness of the foam concrete plate is in the range of 10–50 mm, the fractal dimension decreases from 2.65 to 1.17.
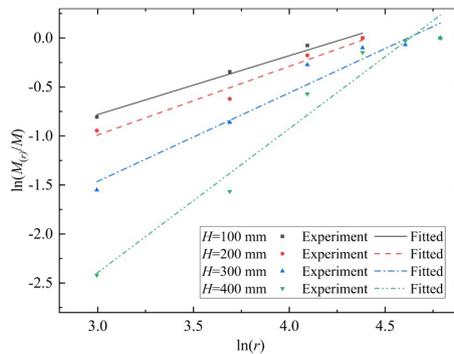

Figure 13 Fractal dimension of foam concrete fragments with different stand-offs
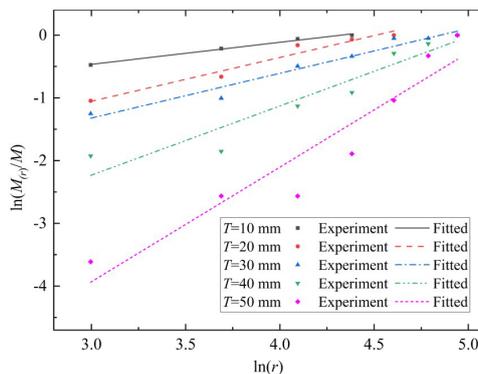

Figure 14 Fractal dimension of foam concrete fragments with different plate thicknesses

Table 4 Calculation results of fractal dimension of foam concrete fragments

Experimental number	Fractal dimension	Relevance
1	2.40	0.9856
2	2.30	0.9672
3	2.10	0.9536
4	1.53	0.9630
5	2.65	0.9924
6	2.30	0.9631
7	2.29	0.9609
8	1.90	0.9077
9	1.17	0.9023

To describe the influence of stand-off and plate thickness on the fragmentation fractal dimension of foam concrete plates quantitatively. In accordance with to the experimental results, the relationships between the stand-off, plate thickness and the fragmentation fractal dimension of the foam concrete plate are fitted, as shown in Figures 15 and 16. From the fitted results, the fragmentation fractal dimension of the foam concrete plate under explosion loading decreases linearly with the increase in stand-off and plate thickness. The degree of fragmentation also decreases. The results are consistent with the statistical characteristics of fragment size.
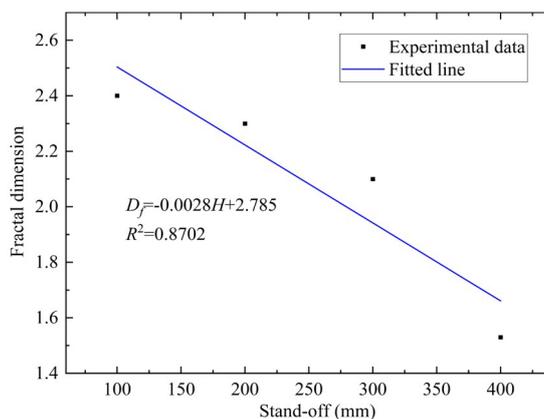
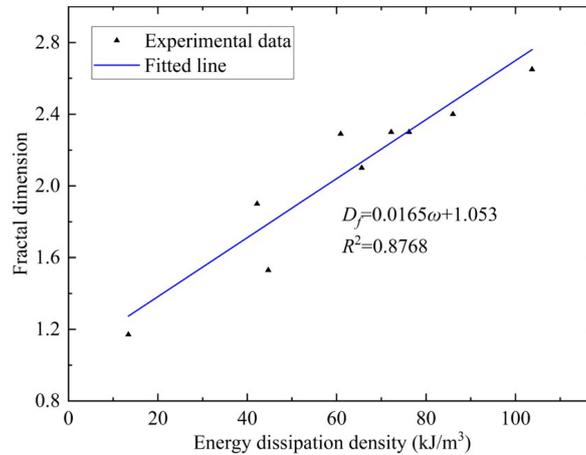**Figure 15** Relationship between fragmention fractal dimension and stand-off
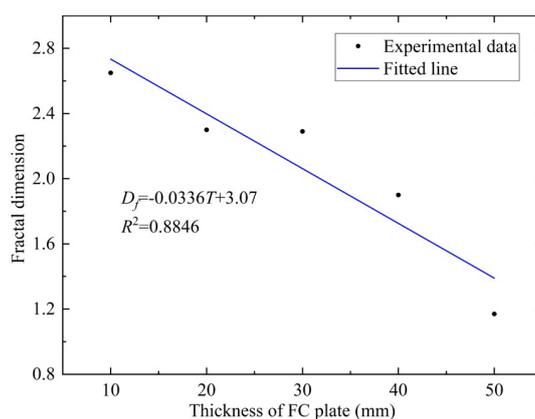
Figure 16 Relationship between fragmention fractal dimension and plate thickness

4.3 Energy dissipation density and fragmentation fractal dimension

The fragmentation energy under explosion loading is intrinsically related to the fragmentation fractal dimension. Figure 17 shows the relationship between fragmentation fractal dimension and energy dissipation density of the foam concrete plate. The results indicate that the fragmentation fractal dimension of foam concrete increases with the increase in energy dissipation density. The larger the energy consumption density in fragmentation is, the more energy

dissipated by the unit volume fragmentation of foam concrete is, and the smaller the size of the fragments generated is. In accordance with the linear relationship fitted in Figure 17, the energy dissipation of foam concrete can be quickly calculated when the size distribution of fragments and the volume of fragmentation zone are known.

Figure 17 Relationship between fragmention fractal dimension and energy dissipation density

5 CONCLUSIONS

In this paper, fragmentation fractal dimension is introduced into the energy dissipation study of foam concrete plates under explosion loading, and an engineering calculation model of foam concrete fragmentation fractal dimension and energy dissipation density is established. The fragmentation fractal dimension is obtained through the statistical analysis of foam concrete fragments collected from explosion experiments, and the energy dissipation in fragmentation is calculated on the basis of plate fracture theory. The research results have important reference significance for the anti-explosion design of engineering facilities and the damage prediction of foam concrete coated structures under explosion loading. The main conclusions of this study are as follows:

1) The fragmentation process of the foam concrete plate under explosion loading is that radial cracks first occur on the plate plane, and then circumferential and shear cracks are generated. The staggered crack network divides the foam concrete plate into fragments of different sizes. The size of the fragments in the central area of the plate is small, and it gradually increases along the radial direction. The results of explosion experiments are consistent with the results of plate fracture theory analysis.

2) The fragment size distribution of foam concrete plates has self-similarity under explosion loading, which is a fractal in a statistical sense. The results of fractal dimension analysis are consistent with the statistical results of fragment size, which verifies the fractal evolution characteristics of foam concrete fragmentation process and the correctness of the calculation model of fragmentation fractal dimension and energy dissipation of foam concrete.

3) The fractal dimension of foam concrete plates can quantitatively reflect the degree of fragmentation. The larger the fractal dimension is, the higher the degree of fragmentation is, and the smaller the size of fragments is. When the stand-off is in the range of 100–400 mm, the fractal dimension is reduced from 2.40 to 1.53. When the plate thickness is in the range of 10–50 mm, the fractal dimension is reduced from 2.56 to 1.17. The fragmentation fractal dimension decreases linearly with the stand-off and plate thickness.

4) The linear relationship between the energy dissipation density and fragmentation fractal dimension of foam concrete plates are $D_f = 0.0165\omega + 1.053$. Therefore, with the increase in stand-off and plate thickness, the size of fragments increases, the fractal dimension of fragments decreases, and the energy dissipation density of foam concrete plates decreases linearly. The energy dissipation is equal to the product of energy dissipation density and fragmentation volume. Under certain loading conditions, the plate thickness with the highest energy dissipation efficiency can be found.

Author's Contributions: Writing - original draft, Wei Shang; Test technical support, Xudong Zu, Zhengxiang Huang, Writing - review & editing, Xudong Zu, Xin Jia, Qiangqiang Xiao; Supervision, Zhengxiang Huang

Editor: Marcílio Alves

Reference

Alan T. Zehnder (2012). Fracture Mechanics. Springer, New York, 7-32.

Alhadid M M A, Soliman A M, Nehdi M L, et al (2014). Critical overview of blast resistance of different concrete types. Magazine of Concrete Research. 66(2): 72-81.

ASTM. E756–05 (2017). Standard Test Method for Measuring Vibration-Damping Properties of Materials. United States.

ASTM. E1820–11 (2012). Standard Test Method for Measurement of Fracture Toughness. United States.

Carpinteri A, Lacidogna G, Pugno N (2004). Scaling of energy dissipation in crushing and fragmentation: a fractal and statistical analysis based on particle size distribution. International journal of fracture. 129(2): 131-139.

Chao X, Tian W, Xu F, et al (2021). A fractal model of effective mechanical properties of porous composites. Composites Science and Technology. 213: 108957.

Edward F. O., Shen W. G., Hamlin M. J., et al (2012). Development of Frangible Concrete to Reduce Blast-Related Casualties. Aci Materials Journal. 109(1):31-40.

Feng S, Zhou Y, Wang Y, et al (2020). Experimental research on the dynamic mechanical properties and damage characteristics of lightweight foamed concrete under impact loading. International Journal of Impact Engineering. 140: 103558.

Fu Y, Zhang Q (2007). Calculating Dynamic Parameters in Elastic Thin Plates Under Blast Loading. Explosion and Shock Waves. 07: 572-575.

Grady D E (1990). Particle size statistics in dynamic fragmentation. Journal of Applied Physics. 68(12): 6099-6105.

Hu X. Z., Wittmann F. H (1992). Fracture energy and fracture process zone. Materials and Structures. 25: 319–326.

Ji J, Li H, Wu F, et al (2020). Fractal characteristics of rock fragmentation under impact load. Journal of Vibration and Shock. 39(13): 176-183.

Kim J, Chung S, Han T, et al (2020). Correlation between microstructural characteristics from micro-CT of foamed concrete and mechanical behaviors evaluated by experiments and simulations. Cement and Concrete Composites. 112: 103657.

Kinney, G.F., Grahm, K.J (1985). Explosive shocks in air. Springer, New York, 88-106.

Kolluru V. L., Yiannis A (2013). Blast Response of Cellular Cement Foams: An Experimental Evaluation. Proceedings of the Fifth Biot Conference on Poromechanics.

Li Y, Dang F, Zhou M, et al (2021). Analysis of Fractal and Energy Consumption Characteristics of Concrete under Impact Loading. Geofluids. 2021: 1-12.

Lei Z, Zhang Z, Huang Y, et al (2021). An investigation of energy consumption variation in rock blasting breaking with the resistance line. Explosion and Shock Waves. 41(07): 151-160.

Ministry of housing and urban rural development of the people s republic of china (2019). GB/T 50081-2019, Standard for test methods of concrete physical and mechanical properties. Beijing: China Standards Press.

Nian W, Subramaniam K V L, Andreopoulos Y (2016). Experimental investigation on blast response of cellular concrete. International Journal of Impact Engineering. 96: 105-115.

Ramamurthy K, Kunhanandan Nambiar E K, Indu Siva Ranjani G (2009). A classification of studies on properties of foam concrete. Cement and Concrete Composites. 31(6): 388-396.

Rudolph Szilard (2004). Theories and Applications of Plate Analysis. Willy, New Jersey, 23-61.

Shen W, Zhang C, Yang Z, et al (2014). Investigation on the safety concrete for highway crash barrier. Construction and Building Materials. 70: 394-398.

Shi Y, Wang J, Cui J (2020). Experimental studies on fragments of reinforced concrete slabs under close-in explosions. International Journal of Impact Engineering. 144: 103630.

Tian X, Li Q, Lu Z, et al (2016). Experimental study of blast mitigation by foamed concrete. International Journal of Protective Structures. 7(2): 179-192.

Turcotte D. L (1986). Fractals and fragmentation. Journal of geophysical research. 91(2): 1921-1926.

Wang X, Zhang X, Song L, et al (2021). Mitigating confined blast response of buried steel box structure with foam concrete. Thin-Walled Structures. 169: 108473.

Wang Y H, Tham L G, Cheung Y K (2005). Beams and plates on elastic foundations: a review. Progress in structural engineering and materials. 7(4): 174-182.

Xie H P (1996). Fractal rock mechanics. Beijing: Science Press, 168-257.

Xu J Y, Fan J S (2012). Dynamic mechanical properties of rock under confining pressure. Xi'an: Northwestern Polytechnical University Press, 135-169.

Xu X, He M, Zhu C, et al (2019). A new calculation model of blasting damage degree—Based on fractal and tie rod damage theory. Engineering Fracture Mechanics. 220: 106619.

Yang J, Jin Q K, Huang F L (1999). Theoretical model and numerical calculation of rock blasting. Beijing: Science Press, 39-54.

Zhang Z Q, Yang J L (2015). Improving safety of runway overrun through foamed concrete aircraft arresting system: an experimental study. International journal of crashworthiness. 20(5): 448-463.

Zhao W S, Chen W Z, Tan X J, et al (2013). Study on foamed concrete used as seismic isolation material for tunnels in rock. Materials research innovations. 17(7): 465-472.